The *JCAD* gene at the 10p11 coronary artery disease locus regulates Hippo signaling in endothelial cells

Peter D. Jones[1,2], Michael A. Kaiser[1,2], Maryam Ghaderi Najafabadi[1,2], Simon Koplev[3], Yuqi Zhao[4], Gillian Douglas[5], Theodosios Kyriakou[5,6], Sarah Andrews[1,2], Rathinasabapathy Rajmohan[1,2], Hugh Watkins[5], Keith M. Channon[5], Shu Ye[1,2], Xia Yang[4], Johan L. M. Björkegren[3,7,8], Nilesh J. Samani[1,2] and Tom R. Webb[1,2,*].

[1] Department of Cardiovascular Sciences, Glenfield Hospital, University of Leicester, Leicester, LE3 9QP, UK.
[2] NIHR Leicester Cardiovascular Biomedical Research Centre, Glenfield Hospital, University of Leicester, Leicester, LE3 9QP, UK.
[3] Department of Genetics and Genomic Sciences, Icahn Institute for Genomics and Multiscale Biology, Icahn School of Medicine at Mount Sinai, One Gustave L. Levy Place - Box 1498, New York, NY 10029-6574, USA.
[4] Department of Integrative Biology and Physiology, University of California, Los Angeles, CA 90403, USA.
[5] British Heart Foundation Centre for Research Excellence, Division of Cardiovascular Medicine, Radcliffe Department of Medicine, Wellcome Trust centre for Human Genetics, University of Oxford, OX3 9DU, UK.
[6] Wellcome Trust Centre for Human Genetics, University of Oxford, Oxford OX3 7BN, UK.
[7] Integrated Cardio Metabolic Centre, Department of Medicine, Karolinska Institutet, Karolinska Universitetssjukhuset, Huddinge, Sweden.
[8] Department of Physiology, Institute of Biomedicine and Translation Medicine, University of Tartu, Estonia.

Running title: JCAD Regulates Hippo Signaling

Corresponding author: Tom R. Webb, Department of Cardiovascular Sciences, Glenfield Hospital, University of Leicester, Leicester, LE3 9QP, UK. Tel: +44 116 204 4762. E-mail: tw126@le.ac.uk

Keywords: Coronary artery disease, Hippo pathway, YAP/TAZ, Endothelium

Subject codes: Coronary Artery Disease, Endothelium/Vascular Type/Nitric Oxide, Cell Biology/Structural Biology, Cell Signaling/Signal Transduction

Word count: 7500

Total number of figures and tables: 10 figures (including 4 supplemental figures), 4 supplemental tables.

TOC category: Basic

TOC subcategory: Arteriosclerosis

Abstract

Objective
A large number of genetic loci have been associated with risk of coronary artery disease (CAD) through genome-wide association studies, however, for most loci the underlying biological mechanism is unknown. Determining the molecular pathways and cellular processes affected by these loci will provide new insights into CAD pathophysiology and may lead to new therapies. The CAD-associated variants at 10p11.23 fall in *JCAD*, which encodes an endothelial junction protein, however, its molecular function in endothelial cells is not known. In this study we characterize the molecular role of JCAD in endothelial cells.

Approach and Results
We show that *JCAD* knockdown in endothelial cells affects key phenotypes related to atherosclerosis including proliferation, migration, apoptosis, tube formation and monocyte binding. We demonstrate that JCAD interacts with LATS2 (large tumor suppressor kinase 2) and negatively regulates Hippo signaling leading to increased activity of YAP (Yes-associated protein), the transcriptional effector of the pathway. We also show by double siRNA knockdown that the phenotypes caused by *JCAD* knockdown require LATS2 and that JCAD is involved in transmission of RhoA-mediated signals into the Hippo pathway. In human tissues, we find that the CAD-associated lead variant, rs2487928, is associated with expression of *JCAD* in arteries, including atherosclerotic arteries. Gene co-expression analyses across disease-relevant tissues corroborate our phenotypic findings and support the link between JCAD and Hippo signaling.

Conclusions
Our results show that JCAD negatively regulates Hippo signaling in endothelial cells and we suggest that JCAD contributes to atherosclerosis by mediating YAP activity and contributing to endothelial dysfunction.

Non-standard abbreviations and acronyms

CAD	coronary artery disease
EC	endothelial cell
HUVEC	human umbilical vein endothelial cells
ICAM1	intercellular adhesion molecule 1
JCAD	junctional protein associated with coronary artery disease
LATS2	large-antigen tumor suppressor
NTC	non-targeting control
TAZ	transcriptional coactivator with PDZ-binding motif
YAP	yes-associated protein

Introduction

Coronary artery disease (CAD), caused by the development of atherosclerotic plaques in the artery wall, is the leading cause of death in the world[1]. Plaques, which tend to localize to sites of disturbed blood flow such as bifurcations and curvature, form as a result of chronic exposure of the arterial endothelium to cardiovascular risk factors and pro-inflammatory factors[2]. The resulting endothelial dysfunction results in expression of adhesion molecules inducing recruitment of inflammatory cells to the site of injury alongside an increase in endothelial permeability and accumulation in lipids in the intima. Subsequently, monocytes migrate into the vessel wall where they differentiate into macrophages, ingest lipids and become foam cells[2, 3]. Advanced atherosclerotic plaques consist of a central core containing lipid-laden cells and extracellular deposits released from dead cells, covered by a fibrous cap consisting primarily of smooth muscle cells and connective tissue. Rupture or erosion of the fibrous cap causes thrombus formation and occlusion of the coronary arteries resulting in myocardial infarction[2].

Several individual characteristics and life style factors including hypertension, elevated low density lipoprotein (LDL) cholesterol, diabetes mellitus and smoking contribute to risk of CAD. There is also a strong genetic determination[4] and in the last decade an increasing number of chromosomal loci have been associated with CAD through genome-wide association studies[5-10].The elucidation of underlying biological mechanisms will provide a better understanding of CAD and has the potential to lead to the development of novel therapeutics directed against processes not targeted by current treatments.

In this context, the CAD genome-wide associated variants at the 10p11.23 locus lie within *JCAD (Junctional Cadherin-5 Associated Protein)* gene, previously known as *KIAA1462* and *Junctional Protein Associated with CAD*, which encodes a protein which localizes to endothelial cell (EC) junctions[11] and regulates angiogenesis[12], however, the molecular role of JCAD in ECs has not been examined. Two independent proteomic studies have previously identified JCAD as an interactor of members of the human Hippo signaling pathway[13, 14] and during the preparation of this manuscript, Ye *et al.* reported that JCAD acts as an inhibitor of a core Hippo signaling protein in liver cancer[15]. The Hippo pathway promotes cell death and differentiation and inhibits cell proliferation[16] in response to various signals including cell contact, mechanotransduction signals and GPCR mediated signaling[17]. A kinase cascade controls the nuclear localization of two homologous transcriptional co-activators of the pathway; YAP (Yes-associated protein) and TAZ (transcriptional coactivator with PDZ-binding motif)[18]. When the Hippo pathway is activated, MST1 and 2 (mammalian STE20-like protein kinase 1 and 2) phosphorylate LATS1 and 2 (large antigen tumor suppressor 1 and 2), which in turn phosphorylate YAP/TAZ resulting in them being bound by 14-3-3 proteins, excluded from the nucleus and subsequently degraded[16, 18]. Therefore, when the Hippo pathway is inactive, YAP/TAZ enter the nucleus and bind to the TEAD1-4 (TEA domain transcription factor 1-4) transcription factors, promoting expression of downstream genes.

YAP/TAZ are key regulators of EC function and are essential for angiogenesis and vascular homeotsasis[19, 20]. Notably, two recent studies have produced compelling evidence that YAP/TAZ activity is a critical mediator of endothelial dysfunction and atherogenesis at sites of disturbed blood flow and in response to inflammatory cytokines[20,21]. Unidirectional blood flow, which is important for normal vascular function and is atheroprotective, was shown to signal through Integrin-β3 and inhibit the small GTPase RhoA, suppressing YAP/TAZ activity. Atherogenic disturbed flow induced YAP/TAZ activity and mediated a proinflammatory response, promoting endothelial adhesion molecule expression and monocyte adhesion[21, 22]. In *Apoe*$^{-/-}$ mice, inhibition of YAP by injection of morpholino oligonucleotides[21] or EC-specific CRISPR/Cas YAP knockdown[22] reduced plaque size in

partial carotid ligation disturbed flow models. EC-specific YAP overexpression increased atherosclerosis[22]. Interestingly, YAP/TAZ, via RhoA, have been identified as mediators of the athero-protective and anti-inflammatory effects of statins[23, 24]. Statin treatment of ECs caused inhibition of YAP/TAZ activity and blocked EC atherosclerotic phenotypes, suggesting that Hippo signaling and YAP/TAZ might be viable targets for new therapeutics[21, 22].

Here, we present our investigation of *JCAD* and its function in ECs. We demonstrate that JCAD is required for normal EC function, interacts with LATS2 and promotes YAP/TAZ activity by acting as a negative regulator of Hippo signaling in ECs. We show that JCAD is required for regulation of Hippo signaling by RhoA and that the phenotypic effects of JCAD require LATS2. We use translational network analysis of gene expression in disease relevant human tissues to corroborate our findings.

Materials and Methods

All data that support the findings of this study are either available within the article, the supplemental material or are available from the corresponding author upon reasonable request.

Cell culture, siRNA and drug treatments
HUVECs were obtained from Promocell. Three independent lines were used for all experiments. HUVECs were cultured in Endothelial Cell Growth Medium MV (Promocell). To knock-down *JCAD*, 2 unique siRNAs (Qiagen, SI04210136, SI04344704) were reverse transfected into the cells using RNAiMAX transfection reagent (Life Technologies, 10514953), *LATS2* knockdown was achieved using a Dharmacon Smart pool of 4 siRNAs (GE Life Sciences, L-003865-00-0005). HAECs were cultured in EGM-2 media (Lonza, CC-3156) and *JCAD* knockdown achieved with a Dharmacon Smart pool of 4 siRNAs (GE Life Sciences, L-026476-02-0005), also transfected using RNAiMAX.Thp-1s were cultured in RPMI (Corning, 10-040-CVR) supplemented with 10% FBS. HEK293A cells were cultured in DMEM with 10% FBS. Drug treatments were carried out in full Endothelial media, for 1 hour treatment time, TRAP6 (Sigma-Aldrich, T1573) was used at 1 μM and Y-27632 (Stemcell Technologies, 72304) at 10 μM.

Proliferation, apoptosis, migration and tube formation assays
For proliferation assays, HUVECs were seeded in 96-well plates at $2x10^3$ cells/well, with 8 replicates per sample. The sulforhodamine-B assay was used. HAECs were seeded at $5x10^3$ cells/well, fixed with 4% paraformaldehyde after 72 hours, DAPI stained and imaged using an Operetta imaging system (Perkin-Elmer, HH12000000). Apoptosis was measured by staining with Annexin-V-FITC (Biolegend, 640906) and measured with a Cyan ADP Flow Cytometer (Beckman Coulter, no catalog number) using standard methods. Cell migration was measured using a wound-healing assay. Cells were grown in a 24-well plate until confluent, then a scratch created across the whole well using a pipette tip. A Nikon Eclipse Ti microscope equipped with an LED light source for epifluorescence and a Nikon Perfect Focus System at the Advanced Imaging Facility of the University of Leicester was used to record images every hour. The microscope has an environmental chamber with temperature control and CO2 supply. An Andor iXonEM+ EMCCD DU 885 camera is attached to the microscope for image collection using NIS-Elements software (Nikon Instruments Europe). Tube formation was carried out in Ibidi angiogenesis slides. Matrigel (Corning, 354277) was plated into the well, allowed to polymerise for 1 hour, then 10^4 cells were added to each well. After 6 hours, images were taken of each well at 4x magnification using an EVOS Fluorescent Microscope (Fisher Scientific) or Nikon Eclipse TE2000-U. The FIJI distribution of ImageJ[25] with the plugin Angiogenesis Analyzer was used to measure the total tubule length in each image.

JCAD-GFP cloning, expression and immunoprecipitation
The full-length open reading frame (ORF) of *JCAD* in the pF1K vector was obtained from Promega. The full ORF was PCR amplified from this, and subcloned into the pLEICS-29 vector by the Protein Expression Laboratory at the University of Leicester. JCAD-GFP or empty pLEICS-29 expressing GFP alone were transfected into HUVECs using Lipofectamine-LTX transfection reagent (Life Technologies, A12621). Cells were then trypsinised, lysed in protein lysis buffer (10 mM Tris-HCl pH 7.5, 150 mM NaCl, 0.5 mM EDTA and 0.5% NP-40) with Roche cOmplete protease inhibitor cocktail (Sigma-Aldrich, 4693159001) and Roche PhosSTOP phosphatase inhibitors (Sigma-Aldrich, 4906845001). Immunoprecipitation was carried out using GFP-Trap A beads (Chromotek, gta-10) according to the manufacturer's instructions.

Western blotting
Cells were lysed in protein lysis buffer (10 mM Tris-HCl ph 7.5, 150 mM NaCl, 0.5 mM EDTA and 0.5% NP-40). Western blotting was carried out using the NuPAGE electrophoresis system (Life Technologies, NP0335BOX) according to standard procedures. Primary antibodies used were Anti-LATS2 at 1 µg/ml (NEB), Anti-phospho-YAP at 1 µg/ml (NEB, 13008S), anti-YAP at 1 µg/ml (NEB, 4912S) and anti-β-actin at 0.56 µg/ml (abcam, ab2676). Secondary anti-mouse IgG (NEB, 7076S) and anti-rabbit IgG (NEB, 7074S) were used at 0.067 µg/ml

Immunofluoresence and microscopy
Cells were grown on Ibidi µ-slide chamber slides until the right level of confluence was obtained. Cells were then fixed with 4% paraformaldehyde, permeabilised with Triton-X-100, then stained according to standard procedures. Anti-YAP was used at 10 µg/ml (NEB, 4912S). Anti-JCAD was used at 4 µg/ml (Sigma-Aldrich, HPA017956). Images were obtained using an inverted Leica TCS SP5 confocal microscope with an x63 oil immersion objective at the Advanced Imaging Facility of the University of Leicester.

Gene expression analysis
RNA was extracted from cells using an RNeasy miniprep kit (Sigma-Aldrich, 74104), reverse transcribed with Superscript III (Fisher Scientific, 18080093) and qPCR carried out using Sensimix (Bioline, QT650-05) on a Rotorgene Q qPCR machine (Qiagen, 9001550).

Monocyte adhesion assay
THP-1 monocytes were cultured in RPMI-1640 medium supplemented with 10% FBS and 1% penicillin-streptomycin. Cells were pelleted, resuspended to a concentration of 1 x 10^5 cells/ml in full medium. Cells were labelled with 5mM Calcein-AM (Fisher Scientific, C3099) for 30 minutes. The HUVEC monolayers were treated with TNFα (R&D Systems, 210-TA-005) for 30 minutes as appropriate, washed with RPMI-1640, then 1x10^4 THP-1 cells added and incubated for 30 minutes. The THP-1s were then removed and the THP-1-bound monolayer washed 4 times with RPMI-1640. The final wash was removed, then the cells fixed with 4% paraformaldehyde. Images were taken with an EVOS Fluorescent Microscope (Fisher Scientific) and the number of bound cells counted manually in ImageJ.

ICAM-1 Flow cytometry
Cells were stained in staining buffer (PBS, pH 7.2, 0.5% bovine serum albumin, 2mM EDTA) with 1:10 diluted anti-CD54-APC (Miltenyi Biotec, 130-103-840) for 20 minutes in the dark at 4°C. Cells were then analysed using Cyan ADP Flow Cytometer (Beckman Coulter) using standard methods.

Network analysis
The RNA-seq expression profiles in 44 tissues (n≥50; subcutaneous adipose, artery, etc.) were retrieved from Genotype-Tissue Expression (GTEx) database[26]. To construct the tissue-specific co-expression networks, we used Multiscale Embedded Gene Co-expression

Network Analysis (MEGENA, v1.3.6)[27] with default parameters. Benjamini-Hochberg False Discovery Rate (FDR)[28] threshold <0.05 was used to define the significant coexpression modules. For STARNET, normalized gene expression data were analyzed using block-wise weighted gene correlation network analysis (WGCNA) with two distinct beta values for within- and between-tissue correlations: 5.2 and 2.7. To infer Bayesian networks within each co-expression module, we used a Fast Greedy Equivalence Search algorithm[29] implemented in the rcausal R package developed by the Center for Causal Discovery. Key driver analysis on the inferred Bayesian networks was performed using the mergeomics R package.

Statistical Analysis
Statistical analyses were carried out using R software version 3.4[30] and GraphPad Prism (GraphPad software).Flow cytometry data was analysed using a custom script utilizing the flowCore and flowStats Bioconductor packages for R[31, 32]. The number of biological replicates is shown in all figures and each experiment was carried out in technical triplicate or quadruplicate. Student's *t* test were used to test for differences of the mean between specific siRNAs and the control. Groups were tested for normality using the Shapiro-Wilk test and for equal variance using the F-test to ensure validity of the t-test. . Proliferation data was analysed using a linear mixed model in R, incorporating sample group and time as fixed effects and sample replicates as random effects. Specific group mean differences were analysed at 24, 48 and 72 hours and adjusted by false discovery rate to account for multiple comparisons. All barcharts represent mean +/- standard deviation. Significance levels are as follows: n.s. $p > 0.05$, * $p \leq 0.05$, ** $p \leq 0.01$, *** $p \leq 0.001$.

Results

JCAD knockdown alters EC function.
To explore the functional role of *JCAD* in ECs we first investigated the cellular consequences of siRNA knockdown of *JCAD* in human umbilical vein endothelial cells (HUVECs) (Fig. 1). We achieved knockdown of 40 to 60% in *JCAD* mRNA levels using 2 independent siRNAs in comparison to non-targeting control (NTC) siRNA (Fig 1A). We measured proliferation of *JCAD* knockdown cells compared to control and found a reduction in cell number in *JCAD* knockdown cells of approximately 15% after 48 hours (siRNA1 $p<0.001$, siRNA2 $p<0.001$)(Fig 1B). We found a similar decrease in proliferation in human aortic endothelial cells (HAECs) following *JCAD* knockdown ($p=0.048$) (Supplemental Figure II) suggesting a common role for JCAD throughout the vasculature. Next, we measured the proportion of cells which were apoptotic using flow cytometry with an anti-Annexin-V antibody. There was an increase in the proportion of apoptotic cells of ~50% with both siRNA1 ($p=0.005$) and siRNA2 ($p=0.006$) (Fig 1C). To test the impact of JCAD knockdown on cell migration, we performed an *in vitro* wound-healing assay and measured the rate at which the cells migrated to close the wound. The rate of migration was reduced in *JCAD* knock-down cells, with siRNA1 treated cells migrating ~20% slower in both siRNA1 ($p=0.0001$) and siRNA2 treated cells ($p=0.0001$) compared to NTC siRNA treated cells (Fig 1D). We tested the angiogenic capability of HUVECs following *JCAD* knockdown using a tube formation assay, which relies on the ability of endothelial cells to self-organise into a network of simple tubes when plated onto Matrigel basement membrane matrix. We measured the total length of tubes formed and found a reduction in the tubule length with *JCAD* knock-down of more than 25% compared to NTC siRNA ($p=0.001$ for siRNA and $p=0.0007$ for siRNA2) (Fig 1E and 1F). These phenotypes demonstrate a role for JCAD in regulating EC function – with reduced JCAD expression causing decreased proliferation, migration and angiogenic capability but increased apoptosis.

Increased YAP/TAZ activity i.e. less active Hippo signaling has recently been demonstrated to promote monocyte binding to the endothelium via regulation of adhesion molecule expression[21, 22]. To determine whether *JCAD* is involved in the regulation of monocyte adhesion, we used an *in vitro* assay to examine adhesion of monocytes to siRNA-treated

ECs. The number of monocytes bound to the confluent layer of HUVECs was significantly reduced by approximately 30% with JCAD knock-down (p=0.0001 for siRNA1 and p=0.0007 for siRNA2) (Fig 1G). To investigate the mechanism of altered monocyte adhesion, we measured the level of Intercellular Adhesion Molecule 1 (ICAM1) protein in cells induced with TNFα using flow cytometry (Fig 1H). In cells treated with siRNA1, ICAM1 protein level was reduced by ~12% compared to control siRNA treated cells (p=0.001), in siRNA2 treated cells, ICAM1 expression was reduced by ~13% (p=0.0075). We also used qPCR to examine the expression of *ICAM1* as well as *VCAM1 (Vascular Cell Adhesion Molecule 1)* and *SELE (Selectin E)*, two other key adhesion genes expressed in HUVECs. *ICAM1* mRNA level was reduced by ~18% in siRNA1 treated cells (p=0.022) and ~25% in siRNA2 treated cells (p=0.042). *VCAM1* mRNA level was reduced by 25% in siRNA1 treated cells (p=0.022) and 24% in siRNA2 treated cells (p=0.0002). *SELE* mRNA level was reduced by 22% in siRNA1 treated cells (p=0.008), in siRNA2 treated cells, there was also a trend towards a reduction in expression, although this wasn't statistically significant (p=0.092) (Fig 1I). These data show that knock-down of *JCAD* expression in ECs results in decreased adhesion molecule expression and monocyte adhesion.

JCAD promotes YAP activity in ECs

JCAD was recently found to interact with LATS2, a core kinase of the Hippo signaling pathway, in a high-throughput immunoprecipitation-mass spectrometry (IP-MS) screen[13].The Hippo pathway has a key role in regulating various cell phenotypes, including proliferation, migration and apoptosis. Therefore, we sought to determine whether the regulation of EC functions by *JCAD* occurs via regulation of the Hippo signaling pathway. Initially, we sought to confirm the physical interaction of JCAD and LATS2 by immunoprecipitation. We overexpressed both JCAD-GFP and Myc-LATS2 in HEK293A cells, immunoprecipitated Myc-LATS2 and probed for GFP by western blot. GFP alone did not bind to the Myc-LATS2, but JCAD-GFP did (Fig 2A). To determine whether *JCAD* perturbs Hippo signaling, we used western blotting with a phospho-specific anti-YAP (p127) antibody, which detects inhibitory phosphorylation on a serine residue at amino acid position 127 of the Hippo pathway effector YAP. We found an increase in the level of YAP (p127) phosphorylation in *JCAD* knock-down cells compared to NTC control, but no change in total YAP levels (Fig 2B). When the Hippo pathway is active, phosphorylated YAP is excluded from the nucleus. We therefore examined the proportion of nuclear YAP in siRNA treated cells by immunofluorescence with an anti-YAP antibody, and found a reduction in the YAP nuclear/cytoplasmic ratio in JCAD siRNA treated cells (p=0.0001 for siRNA1 and p=0.0008 for siRNA2) (Fig 2C and 2D). The increase in phosphorylated YAP and reduction in nuclear YAP in *JCAD* knockdown cells demonstrate increased activity of the core Hippo pathway and would be expected to result in altered expression of Hippo regulated genes. We therefore examined the expression of 3 genes known to be activated by YAP/TAZ – *CTGF* (Connective Tissue Growth Factor)[33], *CCND1* (Cyclin D1)[34] and *BIRC5* (Baculoviral Inhibitor of apoptosis Repeat-Containing 5)[35] by qPCR following siRNA knockdown of *JCAD*. All 3 genes examined showed reduced expression in *JCAD* knock-down cells compared to control cells (Fig 2E).

JCAD mediates Hippo pathway regulation via RhoA

To further understand the role of *JCAD* in Hippo signaling, we studied the impact of JCAD knockdown on the influence of other regulators of the pathway. In cells that are at low confluency and are therefore actively growing, the Hippo pathway is inactive, and YAP is nuclear and active[16]. RhoA is an important regulator of Hippo signaling and responds to stimuli including cell confluency, mechanotransduction and signaling molecules such as Thrombin[16, 36, 37]. In low confluency cells, treatment with the ROCK (Rho-associated coiled-coil forming protein serine/threonine kinase) inhibitor Y-27632, which suppresses the effects of RhoA and promotes Hippo signaling[37]. In highly confluent cells, the Hippo pathway is active, YAP is excluded from the nucleus and unable to promote expression of regulated genes[16]. In these cells, TRAP6, a synthetic PAR1 (Protease-activated receptor1) agonist, which stimulates thrombin signaling via RhoA, down-regulates Hippo signaling and results

in nuclear YAP and increased expression of regulated genes[36]. To explore the role of JCAD in regulating Hippo signaling we grew HUVECs to be at low confluency (40-50%) and high confluency (95-100%) 48 hours after siRNA knockdown and treated the cells with Y-27632, TRAP6, or mock treatment. We then measured the nuclear/cytoplasmic ratio of YAP by staining with α-YAP. At low confluency YAP localized to the nucleus and TRAP6 had no effect on YAP localization on NTC transfected cells (Fig 3 A and B). At high confluency, TRAP6 caused the nuclear/cytoplasmic ratio of YAP to increase by more than 60% (p=0.039) in NTC transfected cells (Fig 3 A and C). Y-27632 reduced the YAP nuclear/cytoplasmic ratio by approximately 40% (p=0.027) (Fig 3 A and B) in NTC cells at low confluency, but not in high confluency cells (Fig 3 A and C). Knockdown of JCAD resulted in exclusion of YAP from the nucleus and a loss of response to both drugs. This places JCAD in the same part of the pathway as RhoA in the Hippo signaling pathway.

The effects of JCAD knockdown on EC function require LATS2.

Having demonstrated that JCAD regulates Hippo signaling and that it interacts with LATS2 kinase, we sought to demonstrate that the effects of *JCAD* knockdown require functional LATS2 using double siRNA knockdown. Initially, we examined phospho-YAP and YAP levels in siRNA treated endothelial cells and found that the increase in YAP phosphorylation caused by *JCAD* siRNA was abolished by knockdown of *LATS2* expression (Fig. 4A). We then used double siRNA treatments and investigated the same EC phenotypes tested previously. We examined proliferation of endothelial cells and found that where proliferation was reduced with either JCAD siRNA alone, it increased with both LATS2 knockdown and double *JCAD LATS2* knockdown (for siRNA1 vs siRNA1 and siLATS2 and for siRNA2 vs siRNA2 and siLATS2, $p<0.001$ at 48 and 72 hour timepoints). There was no significant difference between the double siRNAs and LATS2 alone (p=0.903 for siRNA1; p=0.241 for siRNA2 at 72 hrs) (Fig. 4B). Migration rate was determined with an *in vitro* wound healing assay, migration rate was increased in both LATS2 and double JCAD LATS2 siRNA samples (p=0.001 for siRNA1; p=0.001 for siRNA2). There was no significant difference between the double siRNAs and LATS2 alone (p=0.700 for siRNA1; p=0.804 for siRNA2) (Fig. 4C). Apoptosis was measured by Annexin-V flow cytometry, and double siRNA treated samples had reduced Apoptosis compared to single *JCAD* siRNA alone (p=0.001 for siRNA1; p=0.001 for siRNA2). There was no significant difference between double siRNA and LATS2 alone (p=0.728 for siRNA1; p=0.702 for siRNA2) (Fig. 4D). Monocyte adhesion was measured and was found to be increased in *LATS2* and *JCAD LATS2* double siRNA treated samples compared to *JCAD* siRNA alone (p=0.002 for siRNA1; p=0.003 for siRNA2). There was no significant difference between double siRNA and *LATS2* alone (p=0.299 for siRNA1; p=0.414 for siRNA2) (Fig 4E). Endothelial tube formation on matrigel was determined and there was increased tube formation in double siRNA treated samples compared to *JCAD* siRNA alone (p=0.004 for siRNA1; p=0.019 for siRNA2). Again, there was no significant difference between double siRNA and *LATS2* siRNA alone (p=0.797 for siRNA1; p=0.337 for siRNA2) (Fig 4F). These data show that the effects of JCAD on EC phenotype require the action of LATS2.

CAD-associated variant in JCAD is associated with JCAD expression in vascular and atherosclerotic tissues in humans

Next, we investigated the transcriptional expression of *JCAD* in 672 CAD patients across 7 tissues (blood, atherosclerotic-lesion free mammary artery (MAM), atherosclerotic aortic root (AOR), subcutaneous fat (SF), visceral abdominal fat (VAF), skeletal muscle (SKLM) and liver (LIV)), measured by RNA-seq in the STARNET study (Stockholm-Tartu Atherosclerosis Reverse Networks Engineering Task)[38] and all tissues in the GTEx (Genotype-tissue Expression) project dataset[39]. In STARNET the lead CAD-associated SNP rs2487928 is a highly significant eQTL (expression quantitative trait locus) for *JCAD* in the arterial wall both in atherosclerotic aortic root (AOR) (p=8.26e-18) and in atherosclerosis free internal mammary artery (MAM) (p=1.26e-34), with the protective allele associated with reduced

expression of *JCAD*. In GTEx, rs2487928 is also a significant eQTL for *JCAD* in aorta (p=1.8e-7). We tested the effects of rs2487928 on endothelial tube formation in a library of HUVECs and observed a trend towards decreased tubule length in cells homozygous for the protective allele compared to risk allele homozygotes, with an intermediate effect in heterozygotes, although this was not statistically significant (Supplemental Figure IV). This is in keeping with the expected effects of reduced *JCAD* expression in the protective genotype. These findings suggest that the protective allele reduces CAD risk through decreased *JCAD* expression in the vessel wall.

Co-expression across human tissues corroborates effects of JCAD on Hippo signaling and endothelial phenotypes

To characterize changes in the expression of other genes associated with expression of *JCAD*, we identified co-expression modules across all STARNET and GTEx tissues using weighted gene correlations analysis (WGCNA)[38] and Multiscale Embedded Gene Co-expression Network Analysis (MEGENA)[40] separately as previously described. *JCAD* was detected in several tissue-specific and cross-tissue modules. We inferred Bayesian networks over the transcripts within modules containing *JCAD* and ran weighted key-driver analysis to detect particularly influential genes. We identified JCAD as a key driver of module 155, which is a cross-tissue module composed mostly of genes from SF and AOR (Fig 5A-D). We then carried out Reactome pathway enrichment analysis on the key drivers to identify significantly over-represented pathways. Notably, "YAP1- and WWTR1 (TAZ)-stimulated gene expression", was identified as an enriched pathway, further supporting the functional link between *JCAD* and Hippo signaling. Other enriched pathways included examples related to Notch signaling and transcriptional regulation by TP53, both of which are downstream of Hippo signaling (Fig 5E)[41, 42]. In addition, JCAD was present in coronary artery module 14 in GTEx and the predominantly MAM-specific module 82 in STARNET (Supplementary Tables I and III). Both of these modules were significantly enriched for GO categories related to the phenotypes detected in our EC experiments including angiogenesis, cell proliferation, apoptosis and adhesion (Supplementary Tables II and IV).

Discussion

The mechanisms by which genes at CAD associated loci identified by genome-wide association studies contribute to disease risk are largely unknown. In this study, we investigated *JCAD*, a largely uncharacterized CAD-associated gene and show that it encodes a LATS2 interacting protein which acts as a new negative regulator of the Hippo signaling pathway in ECs. Notably, recent studies have provided convincing evidence that the activity of YAP/TAZ, the transcriptional effectors of the Hippo pathway, is a key mediator of atherosclerosis at sites of non-linear shear stress and in response to pro-inflammatory cytokines [21, 22]. Our results complement these findings and link the Hippo signaling pathway to CAD in humans via the 10p11 disease association and human gene expression analysis and JCAD function.

We have shown that knock-down of *JCAD* expression induces activation of the Hippo pathway, resulting in an increase in phosphorylated YAP and exclusion of YAP from the nucleus and a decrease in expression of Hippo pathway-regulated genes. This results in the perturbation of a number of important EC phenotypes consistent with known roles of Hippo signaling[16, 21, 22], including increased apoptosis and decreased proliferation, migration and endothelial tube formation. This is in keeping with the known role of the Hippo pathway in these processes[19, 20] and is consistent with a recent study by Hara *et al*., which established a role for JCAD in angiogenesis[12].

The Hippo pathway responds to a number of upstream signals, including mechanical stress, confluency, and G-protein signals via RhoA[16, 36, 43, 44]. Notably, YAP/TAZ are required for

shear stress response and promote atherogenesis in response to disturbed flow, a process which is dependent on RhoA-mediated signals[21]. We found that JCAD is involved in the transmission of signals to the Hippo signaling pathway via RhoA. We have also shown that *JCAD* knockdown reduces YAP nuclear localization in low confluency cells, but not in highly confluent cells, suggesting that JCAD may also be involved in the confluency response of YAP/TAZ, which also acts via RhoA[44]. In addition, we have demonstrated that the phenotypic effects of *JCAD* knockdown in ECs require LATS2, suggesting that these phenotypes are caused by altered regulation of Hippo signaling. Our results are supported by recent work by Ye *et al* who presented evidence that JCAD inhibits LATS2 in liver tumorigenesis by binding to the kinase domain of LATS2[15]. Together, these data identify JCAD as a new regulator of Hippo signaling in both human cardiovascular disease and tumorigenesis.

JCAD is conserved across vertebrates, but lacks known functional domains and has poor homology to other proteins, although there is a short (13 amino acid) region with homology to ROCK 1 and 2 and cingulin proteins[11]. Further studies are needed to determine whether JCAD inhibits LATS2 in response to other signals which regulate the Hippo pathway or whether it is specific to RhoA-mediated signals. Intriguingly, in a recent GWAS[10], variants in the RhoA gene have been associated with CAD risk, providing further evidence that the RhoA-Hippo pathway is involved in the development of CAD.

Co-expression analysis of RNA-seq data from both normal and atherosclerotic human blood vessels support our *in vitro* findings that JCAD regulates EC behavior with modules containing *JCAD* being enriched for GO categories related to cell proliferation, apoptosis, adhesion and angiogenesis. We also found *JCAD* to be a key driver of a cross-tissue module predominantly comprising genes from aorta and subcutaneous fat. Although *JCAD* was a weaker key driver relative to other genes in this co-expression module the identification of YAP/TAZ signaling as an over-represented pathway suggests the module captures relevant biology. It is not clear why *JCAD* and many of the other key drivers are from subcutaneous fat, however, this could be due to the extensive capillary network and high proportion of endothelial cells in adipose tissue[45]. Investigation of other key drivers of this module could potentially identify further novel regulators of Hippo signaling and YAP/TAZ activity.

How CAD-associated variants in *JCAD* affect its function and contribute to disease will require further analysis. We identified an eQTL between the protective allele of the lead SNP, rs2487928, and decreased *JCAD* expression in both atherosclerotic and atherosclerosis-free arterial tissue, suggesting altered transcriptional regulation of *JCAD* as the causal mechanism. Based on our data, we propose a model of the relationship between JCAD and the core Hippo pathway and the how the risk and non-risk alleles alter Hippo signaling (Fig 6). We would expect decreased *JCAD* expression caused by the rs2487928 protective allele to contribute to decreased endothelial dysfunction in response to pro-atherosclerotic signals and decreased monocyte recruitment, resulting in lower macrophage content in atherosclerotic plaques, which could reduce plaque growth and instability. Additionally, promotion of angiogenesis by JCAD could result in increased neovascularization in plaques, higher neovessel density and contribute to plaque growth and instability in this way [46]. *In vivo* models, such as a *JCAD* knockout or overexpressing mouse, will be required to fully determine the role of JCAD in disease pathogenesis. In addition, while we have demonstrated a role for *JCAD* in ECs, but we cannot rule out a role in other cell types and further work should be carried out to investigate this role. In addition endothelial specific targeting of *JCAD* in mice would also improve our understanding of the role of *JCAD* and Hippo signaling in CAD and the contribution of Hippo signaling.

In conclusion, we have demonstrated that the CAD associated gene *JCAD* encodes a novel regulator of Hippo signaling in ECs and suggest that variants at the 10p11.23 CAD locus act

through JCAD to regulate EC function via YAP/TAZ. Future work should assess the therapeutic potential of JCAD and other Hippo pathway components in treating CAD.

Acknowledgements

Author Contributions: P.D.J., G.D., T.K., H.W., K.M.C., S.Y., N.J.S. and T.R.W conceived and designed the experiments. P.D.J., M.A.K., M.G.N., G.D., T.K., S.A. and R.R. carried out the experiments. S.K., Y.Z., X.Y. and J.L.M.B. contributed network data and carried out network and expression analyses. P.D.J., N.J.S. and T.R.W. wrote the manuscript. All authors contributed and commented on the manuscript. We also thank Dr. Mintu Nath for statistical review of the manuscript.

Sources of funding

This work was supported by a Transatlantic Networks of Excellence Award (12CVD02) from The Leducq Foundation. The research leading to these results has received funding from the European Union Seventh Framework Programme FP7/2007-2013 under grant agreement number HEALTH-F2-2013-601456. H.W., K.M.C., N.J.S. and T.R.W. are funded by the British Heart Foundation. K.M.C., H.W. and N.J.S. are UK National Institute for Health Research (NIHR) Senior Investigators. Work was supported by BHF grant PG/15/35/31403 to K.M.C.. Y.Z. and X.Y. are partially supported by the American Heart Association. The DNA genotyping and RNA sequencing in STARNET of which J.L.M.B. is P.I. were in part performed by the SNP&SEQ technology platform at Science for Life, the National Genomics Infrastructure (NGI) in Uppsala and Stockholm supported by Swedish Research Council (VR-RF1), Knut and Alice Wallenberg Foundation and UPPMAX. STARNET has also been supported in part through the computational resources and staff expertise provided by Scientific Computing at the Icahn School of Medicine at Mount Sinai.

Disclosures

J.L.M.B. is the founder and chairman of Clinical Gene Networks.

References

1. GBD 2015 Mortality and Causes of Death Collaborators. Global, regional, and national life expectancy, all-cause mortality, and cause-specifi c mortality for 249 causes of death, 1980–2015: A systematic analysis for the global burden of disease study 2015. *Lancet*. 2016;388:1459-1544
2. Libby P, Ridker PM, Hansson GK. Progress and challenges in translating the biology of atherosclerosis. *Nature*. 2011;473:317-325
3. Tabas I, Garcia-Cardena G, Owens GK. Recent insights into the cellular biology of atherosclerosis. *The Journal of cell biology*. 2015;209:13-22
4. McPherson R, Tybjaerg-Hansen A. Genetics of coronary artery disease. *Circulation research*. 2016;118:564-578
5. CARDIoGRAMplusC4D Consortium, Deloukas P, Kanoni S*, et al.* Large-scale association analysis identifies new risk loci for coronary artery disease. *Nature genetics*. 2013;45:25-33
6. Nikpay M, Goel A, Won HH*, et al.* A comprehensive 1,000 genomes-based genome-wide association meta-analysis of coronary artery disease. *Nature genetics*. 2015;47:1121-1130
7. Myocardial Infarction Genetics Consortium, Kathiresan S, Voight BF*, et al.* Genome-wide association of early-onset myocardial infarction with single nucleotide polymorphisms and copy number variants. *Nature genetics*. 2009;41:334-341
8. Samani NJ, Erdmann J, Hall AS*, et al.* Genomewide association analysis of coronary artery disease. *The New England journal of medicine*. 2007;357:443-453
9. Schunkert H, Konig IR, Kathiresan S*, et al.* Large-scale association analysis identifies 13 new susceptibility loci for coronary artery disease. *Nature genetics*. 2011;43:333-338
10. Nelson CP, Goel A, Butterworth A*, et al.* Support for 243 loci associated with coronary artery disease with data from uk biobank. *Under review*. 2017
11. Akashi M, Higashi T, Masuda S, Komori T, Furuse M. A coronary artery disease-associated gene product, jcad/kiaa1462, is a novel component of endothelial cell-cell junctions. *Biochemical and biophysical research communications*. 2011;413:224-229
12. Hara T, Monguchi T, Iwamoto N*, et al.* Targeted disruption of jcad (junctional protein associated with coronary artery disease)/kiaa1462, a coronary artery disease-associated gene product, inhibits angiogenic processes in vitro and in vivo. *Arteriosclerosis, thrombosis, and vascular biology*. 2017;37:1667-1673
13. Couzens AL, Knight JDR, Kean MJ, Teo G, Weiss A, Dunham WH, Lin Z-Y, Bagshaw RD, Sicheri F, Pawson T, Wrana JL, Choi H, Gingras A-C. Protein interaction network of the mammalian hippo pathway reveals mechanisms of kinase-phosphatase interactions. *Sci Signaling*. 2013;6:rs15
14. Wang W, Li X, Huang J, Feng L, Dolinta KG, Chen J. Defining the protein-protein interaction network of the human hippo pathway. *Molecular & cellular proteomics : MCP*. 2014;13:119-131
15. Ye J, Li TS, Xu G, Zhao YM, Zhang NP, Fan J, Wu J. Jcad promotes progression of nonalcoholic steatohepatitis to liver cancer by inhibiting lats2 kinase activity. *Cancer research*. 2017;77:5287-5300
16. Yu FX, Guan KL. The hippo pathway: Regulators and regulations. *Genes & development*. 2013;27:355-371
17. Meng Z, Moroishi T, Guan KL. Mechanisms of hippo pathway regulation. *Genes & development*. 2016;30:1-17
18. Hansen CG, Moroishi T, Guan KL. Yap and taz: A nexus for hippo signaling and beyond. *Trends in cell biology*. 2015;25:499-513
19. Wang X, Freire Valls A, Schermann G*, et al.* Yap/taz orchestrate vegf signaling during developmental angiogenesis. *Developmental cell*. 2017;42:462-478 e467

20. Choi HJ, Zhang H, Park H, Choi KS, Lee HW, Agrawal V, Kim YM, Kwon YG. Yes-associated protein regulates endothelial cell contact-mediated expression of angiopoietin-2. *Nature communications*. 2015;6:6943
21. Wang KC, Yeh YT, Nguyen P, Limqueco E, Lopez J, Thorossian S, Guan KL, Li YJ, Chien S. Flow-dependent yap/taz activities regulate endothelial phenotypes and atherosclerosis. *Proceedings of the National Academy of Sciences of the United States of America*. 2016;113:11525-11530
22. Wang L, Luo JY, Li B*, et al.* Integrin-yap/taz-jnk cascade mediates atheroprotective effect of unidirectional shear flow. *Nature*. 2016
23. Wang Z, Wu Y, Wang H*, et al.* Interplay of mevalonate and hippo pathways regulates rhamm transcription via yap to modulate breast cancer cell motility. *Proceedings of the National Academy of Sciences of the United States of America*. 2014;111:E89-E98
24. Sorrentino G, Ruggeri N, Specchia V, Cordenonsi M, Mano M, Dupont S, Manfrin A, Ingallina E, Sommaggio R, Piazza S, Rosato A, Piccolo S, Del Sal G. Metabolic control of yap and taz by the mevalonate pathway. *Nature cell biology*. 2014;16:357-366
25. Schindelin J, Arganda-Carreras I, Frise E*, et al.* Fiji: An open-source platform for biological-image analysis. *Nature methods*. 2012;9:676-682
26. Lonsdale J, Thomas J, Salvatore M*, et al.* The genotype-tissue expression (gtex) project. *Nature genetics*. 2013;45:580-585
27. Song WM, Zhang B. Multiscale embedded gene co-expression network analysis. *Plos Comput Biol*. 2015;11
28. Benjamini Y, Hochberg Y. Controlling the false discovery rate - a practical and powerful approach to multiple testing. *J Roy Stat Soc B Met*. 1995;57:289-300
29. Chickering DM. Optimal structure identification with greedy search. *Journal of Machine Learning Research*. 2002;3:507-554
30. R Core Team. R: A language and environment for statistical computing. R foundation for statistical computing, vienna, austria. . 2014
31. Gentleman RC, Carey VJ, Bates DM*, et al.* Bioconductor: Open software development for computational biology and bioinformatics. *Genome biology*. 2004;5:R80
32. Hahne F, LeMeur N, Brinkman RR, Ellis B, Haaland P, Sarkar D, Spidlen J, Strain E, Gentleman R. Flowcore: A bioconductor package for high throughput flow cytometry. *BMC bioinformatics*. 2009;10:106
33. Zhao B, Ye X, Yu J, Li L, Li W, Li S, Yu J, Lin JD, Wang CY, Chinnaiyan AM, Lai ZC, Guan KL. Tead mediates yap-dependent gene induction and growth control. *Genes & development*. 2008;22:1962-1971
34. Cao X, Pfaff SL, Gage FH. Yap regulates neural progenitor cell number via the tea domain transcription factor. *Genes & development*. 2008;22:3320-3334
35. Dong J, Feldmann G, Huang J, Wu S, Zhang N, Comerford SA, Gayyed MF, Anders RA, Maitra A, Pan D. Elucidation of a universal size-control mechanism in drosophila and mammals. *Cell*. 2007;130:1120-1133
36. Mo JS, Yu FX, Gong R, Brown JH, Guan KL. Regulation of the hippo-yap pathway by protease-activated receptors (pars). *Genes & development*. 2012;26:2138-2143
37. Wada K, Itoga K, Okano T, Yonemura S, Sasaki H. Hippo pathway regulation by cell morphology and stress fibers. *Development*. 2011;138:3907-3914
38. Franzen O, Ermel R, Cohain A*, et al.* Cardiometabolic risk loci share downstream cis- and trans-gene regulation across tissues and diseases. *Science*. 2016;353:827-830
39. GTEx Consortium. The genotype-tissue expression (gtex) project. *Nature genetics*. 2013;45:580-585
40. Song WM, Zhang B. Multiscale embedded gene co-expression network analysis. *PLoS Comput Biol*. 2015;11:e1004574

41. Tschaharganeh DF, Chen X, Latzko P*, et al.* Yes-associated protein up-regulates jagged-1 and activates the notch pathway in human hepatocellular carcinoma. *Gastroenterology*. 2013;144:1530-1542 e1512
42. Furth N, Ben-Moshe NB, Pozniak Y, Porat Z, Geiger T, Domany E, Aylon Y, Oren M. Down-regulation of lats kinases alters p53 to promote cell migration. *Genes & development*. 2015;29:2325-2330
43. Low BC, Pan CQ, Shivashankar GV, Bershadsky A, Sudol M, Sheetz M. Yap/taz as mechanosensors and mechanotransducers in regulating organ size and tumor growth. *FEBS letters*. 2014;588:2663-2670
44. Dupont S, Morsut L, Aragona M, Enzo E, Giulitti S, Cordenonsi M, Zanconato F, Le Digabel J, Forcato M, Bicciato S, Elvassore N, Piccolo S. Role of yap/taz in mechanotransduction. *Nature*. 2011;474:179-183
45. Eto H, Suga H, Matsumoto D, Inoue K, Aoi N, Kato H, Araki J, Yoshimura K. Characterization of structure and cellular components of aspirated and excised adipose tissue. *Plastic and reconstructive surgery*. 2009;124:1087-1097
46. Moulton KS. Plaque angiogenesis: Its functions and regulation. *Cold Spring Harb Symp Quant Biol*. 2002;67:471-482

Highlights

- *JCAD*, the candidate gene at the 10p11 locus affects endothelial cell function via the Hippo pathway.
- *JCAD* acts via *LATS2* to regulate YAP activity.
- The protective allele of the lead CAD associated SNP, rs2487928, associates with decreased *JCAD* expression in arteries.

Figure Legends

Figure 1. Phenotypic assessment of *JCAD* knockdown in endothelial cells. (A) qPCR of *JCAD* expression in siRNA treated cells. (B) Cellular proliferation of HUVECs treated with the 3 different siRNAs. N=3 independent knock-downs across 2 independent cell lines. (C) Flow cytometry with an anti-Annexin V antibody was used to determine the proportion of siRNA-treated cells which were apoptotic. N represent independent knock-downs across 2 cell lines. (D) A scratch assay was used to measure the migration rate of siRNA-treated cells. (E and F) For a tube-formation assay, siRNA-treated cells were plated onto Matrigel and incubated for 6 hours. Calcein-AM staining was used for visualisation (D) and total tubule length determined (E). (F) Thp-1 binding to siRNA treated endothelial cells. (G) ICAM1 expression in response to TNFα was measure using flow cytometry. (H) qPCR analysis of expression of adhesion molecule expression. Significance levels: NS $p > 0.05$, * $p < 0.05$, ** $p < 0.01$, *** $P < 0.001$.

Figure 2. *JCAD* knockdown reduces YAP activity. (A) Anti-GFP and Anti-Myc blots on cell lysate and immunoprecipitated Myc-LATS2. (B) Anti-phospho-YAP (p127) western blot on cell lysates from siRNA treated cells. (D) siRNA-treated cells were fixed and stained with Anti-YAP antibody and co-stained with DAPI. (E) Quantification of these images allowed determination of the Nuclear/Cytoplasmic ratio of YAP. (F) qPCR measurement of RNA expression levels of Hippo-pathway regulated genes. Significance levels: NS $p > 0.05$, * $p < 0.05$, ** $p < 0.01$, *** $P < 0.001$.

Figure 3. JCAD is required for the effect of Rho and Thrombin signaling on the Hippo pathway. (A) Quantification of YAP nuclear cytoplasmic ratio in siNTC, siRNA1 and siRNA2 treated HUVECs treated with TRAP6, Y-27632 or untreated. Representative images shown for low confluency (B) and high confluency (C) cells. Significance levels: NS $p > 0.05$, * $p < 0.05$, ** $p < 0.01$, *** $P < 0.001$.

Figure 4. Phenotype assessment of *JCAD LATS2* double siRNA knockdown in endothelial cells. (A) Western blots using of anti-phospho-YAP(p127) and anti-YAP on lysates with *JCAD* and *LATS2* siRNAs. (B) Proliferation, showing statistical comparison between siRNA1 and siRNA1+siLATS2 as well as siRNA2 and siRNA2+siLATS2, (C) Migration, (D) Apoptosis, (E) Monocyte adhesion and (F) tube formation of cells treated with *JCAD* and *LATS2* siRNAs separately and in combination. Significance levels: NS $p > 0.05$, * $p < 0.05$, ** $p < 0.01$, *** $P < 0.001$.

Figure 5 *JCAD* co-expression analysis. (A) Module size and tissue composition of 5 STARNET modules with fewer than 2000 genes which contain *JCAD*. (B) The number of genes in the SF and AOR components and the gene names in the minority tissues in module 155. (C) Inferred bayesian networks showing directed edges involving *JCAD* for each module. (D) The 30 most significant key drivers of module 155 and *JCAD*. (E) Reactome pathway enrichment for all key drivers of module 155.

Figure 6. A model for the effect of *JCAD* CAD risk genotype on the Hippo signaling pathway. The Hippo signaling pathway consists of a core kinase cascade comprising MST1/2 and LATS1/2 and is regulated by multiple extracellular signals. Our data suggests that JCAD acts downstream of RhoA to inhibit LATS2. We propose that in individuals with the non-risk genotype, lower JCAD expression results in more active LATS1/LATS2, increased phosphorylation of YAP/TAZ and its exclusion from the nucleus. Conversely, in individuals with the risk genotype, higher JCAD expression results in lower LATS1/2 activity, reduced YAP/TAZ phosphorylation and more active nuclear YAP, resulting in increased expression of pro-proliferative, anti-apoptotic and pro-inflammatory genes, promoting endothelial dysfunction and atherogenesis.

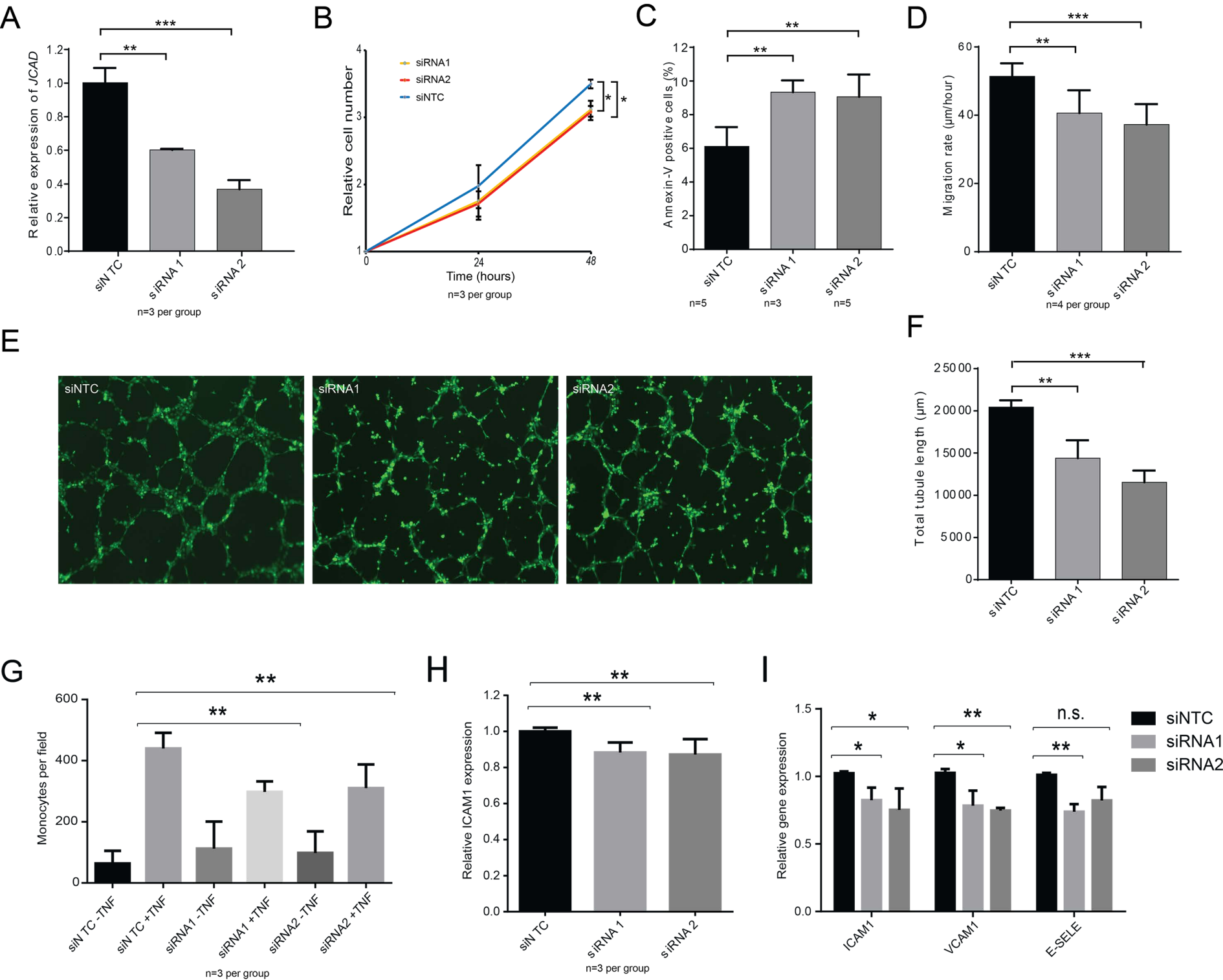
A
Relative expression of JCAD
siNTC
siRNA 1
siRNA 2
n=3 per group
B
Relative cell number
siRNA1
siRNA2
siNTC
Time (hours)
n=3 per group
C
Annexin-V positive cells (%)
siNTC
siRNA 1
siRNA 2
n=5
n=3
n=5
D
Migration rate (μm/hour)
siNTC
siRNA 1
siRNA 2
n=4 per group
E
siNTC
siRNA1
siRNA2
F
Total tubule length (μm)
siNTC
siRNA 1
siRNA 2
G
Monocytes per field
siNTC -TNF
siNTC +TNF
siRNA1 -TNF
siRNA1 +TNF
siRNA2 -TNF
siRNA2 +TNF
n=3 per group
H
Relative ICAM1 expression
siNTC
siRNA 1
siRNA 2
n=3 per group
I
Relative gene expression
ICAM1
VCAM1
E-SELE
n.s.
siNTC
siRNA1
siRNA2

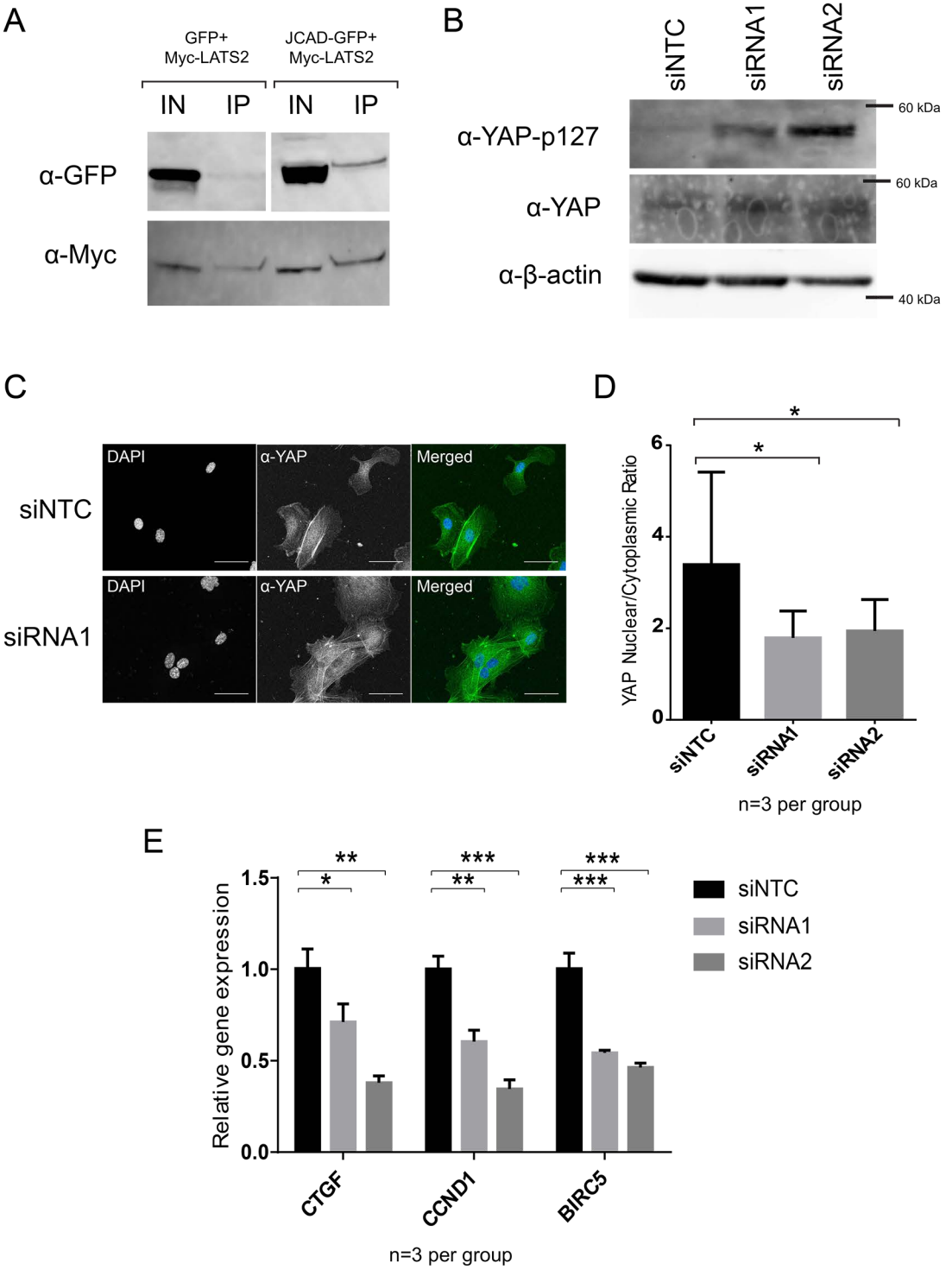
A
GFP+
Myc-LATS2
JCAD-GFP+
Myc-LATS2
IN
IP
IN
IP
α-GFP
α-Myc
B
siNTC
siRNA1
siRNA2
α-YAP-p127
α-YAP
α-β-actin
60 kDa
60 kDa
40 kDa
C
DAPI
α-YAP
Merged
siNTC
siRNA1
D
YAP Nuclear/Cytoplasmic Ratio
siNTC
siRNA1
siRNA2
n=3 per group
E
Relative gene expression
siNTC
siRNA1
siRNA2
CTGF
CCND1
BIRC5
n=3 per group

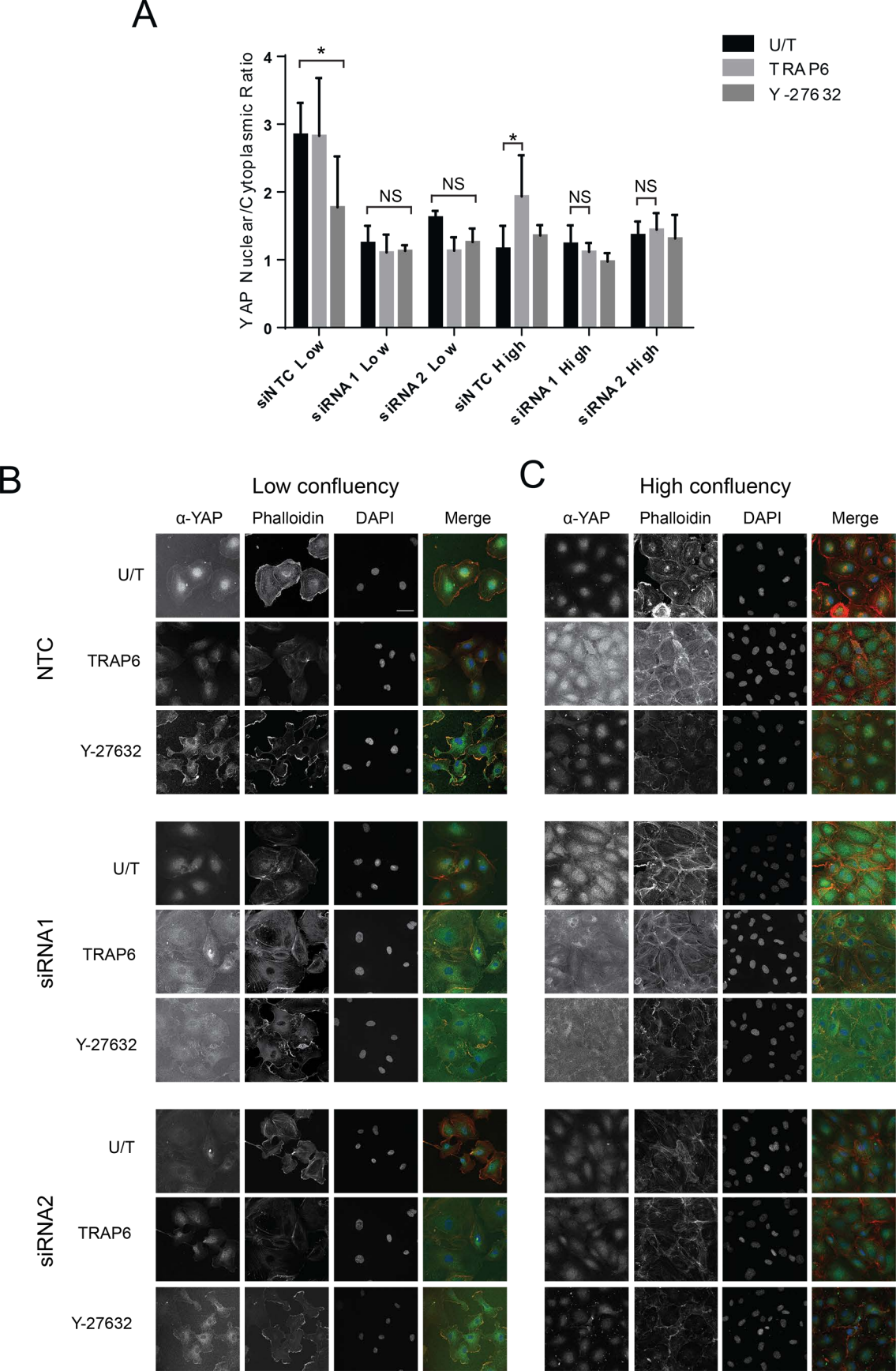
A
U/T
TRAP6
Y-27632
YAP Nuclear/Cytoplasmic Ratio
0
1
2
3
4
*
NS
NS
*
NS
NS
siNTC Low
siRNA1 Low
siRNA2 Low
siNTC High
siRNA1 High
siRNA2 High
B
Low confluency
C
High confluency
α-YAP
Phalloidin
DAPI
Merge
NTC
siRNA1
siRNA2
U/T
TRAP6
Y-27632

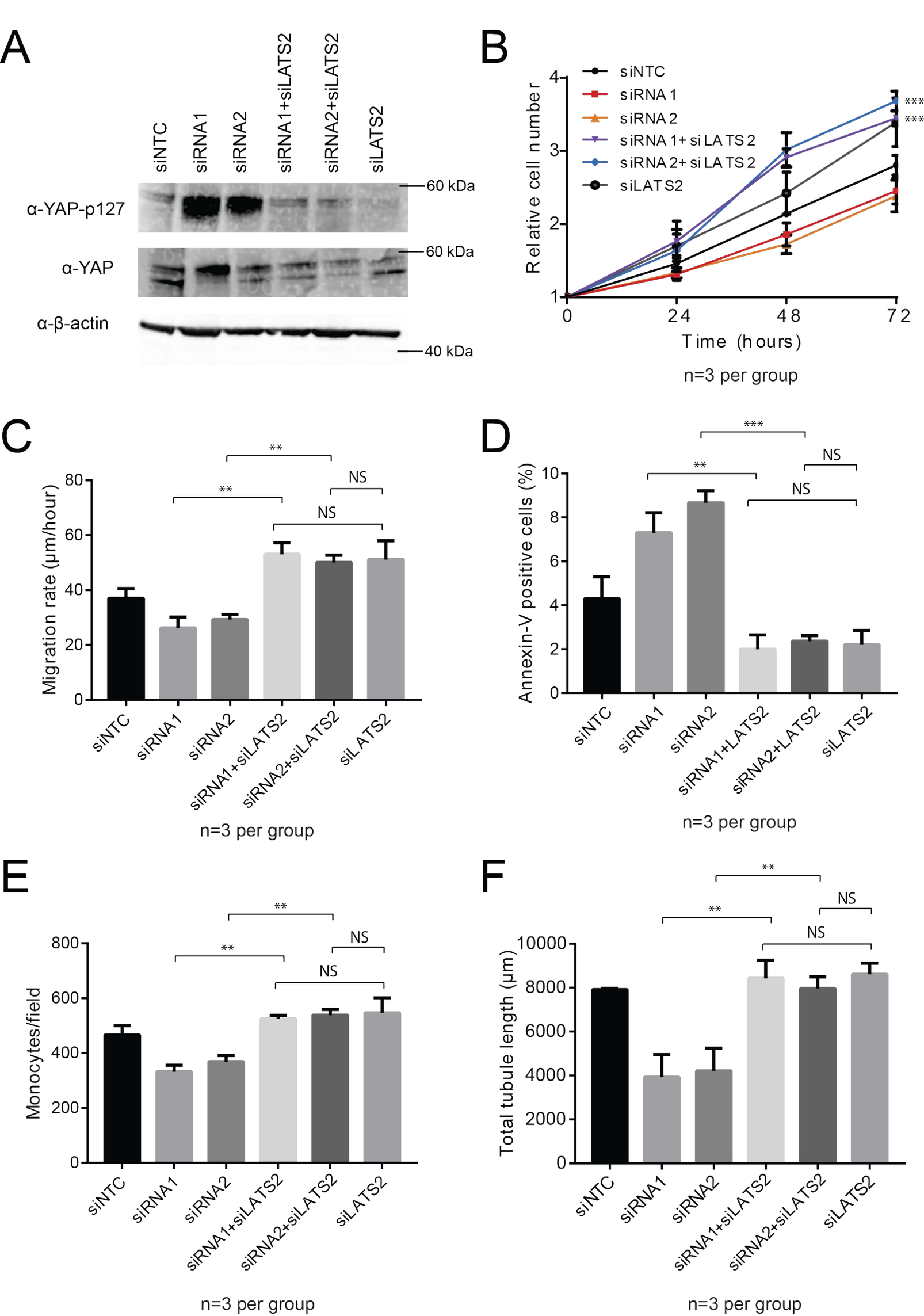
A
siNTC
siRNA1
siRNA2
siRNA1+siLATS2
siRNA2+siLATS2
siLATS2
α-YAP-p127
α-YAP
α-β-actin
60 kDa
60 kDa
40 kDa
B
siNTC
siRNA 1
siRNA 2
siRNA 1+ siLATS2
siRNA 2+ siLATS2
siLATS2
Relative cell number
Time (hours)
0
24
48
72
***
***
n=3 per group
C
Migration rate (μm/hour)
**
**
NS
NS
siNTC
siRNA1
siRNA2
siRNA1+siLATS2
siRNA2+siLATS2
siLATS2
n=3 per group
D
Annexin-V positive cells (%)
***
**
NS
NS
siNTC
siRNA1
siRNA2
siRNA1+LATS2
siRNA2+LATS2
siLATS2
n=3 per group
E
Monocytes/field
**
**
NS
NS
siNTC
siRNA1
siRNA2
siRNA1+siLATS2
siRNA2+siLATS2
siLATS2
n=3 per group
F
Total tubule length (μm)
**
**
NS
NS
siNTC
siRNA1
siRNA2
siRNA1+siLATS2
siRNA2+siLATS2
siLATS2
n=3 per group

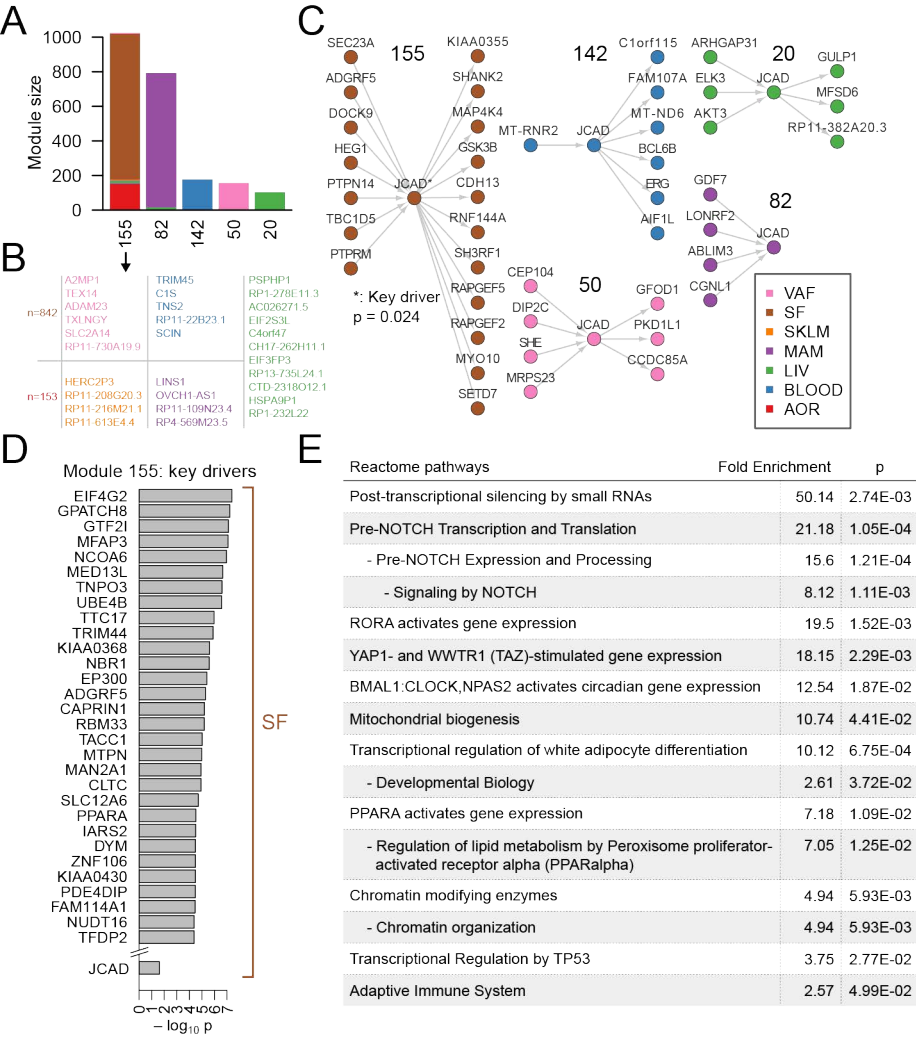

Reactome pathways	Fold Enrichment	p
Post-transcriptional silencing by small RNAs	50.14	2.74E-03
Pre-NOTCH Transcription and Translation	21.18	1.05E-04
- Pre-NOTCH Expression and Processing	15.6	1.21E-04
- Signaling by NOTCH	8.12	1.11E-03
RORA activates gene expression	19.5	1.52E-03
YAP1- and WWTR1 (TAZ)-stimulated gene expression	18.15	2.29E-03
BMAL1:CLOCK,NPAS2 activates circadian gene expression	12.54	1.87E-02
Mitochondrial biogenesis	10.74	4.41E-02
Transcriptional regulation of white adipocyte differentiation	10.12	6.75E-04
- Developmental Biology	2.61	3.72E-02
PPARA activates gene expression	7.18	1.09E-02
- Regulation of lipid metabolism by Peroxisome proliferator-activated receptor alpha (PPARalpha)	7.05	1.25E-02
Chromatin modifying enzymes	4.94	5.93E-03
- Chromatin organization	4.94	5.93E-03
Transcriptional Regulation by TP53	3.75	2.77E-02
Adaptive Immune System	2.57	4.99E-02

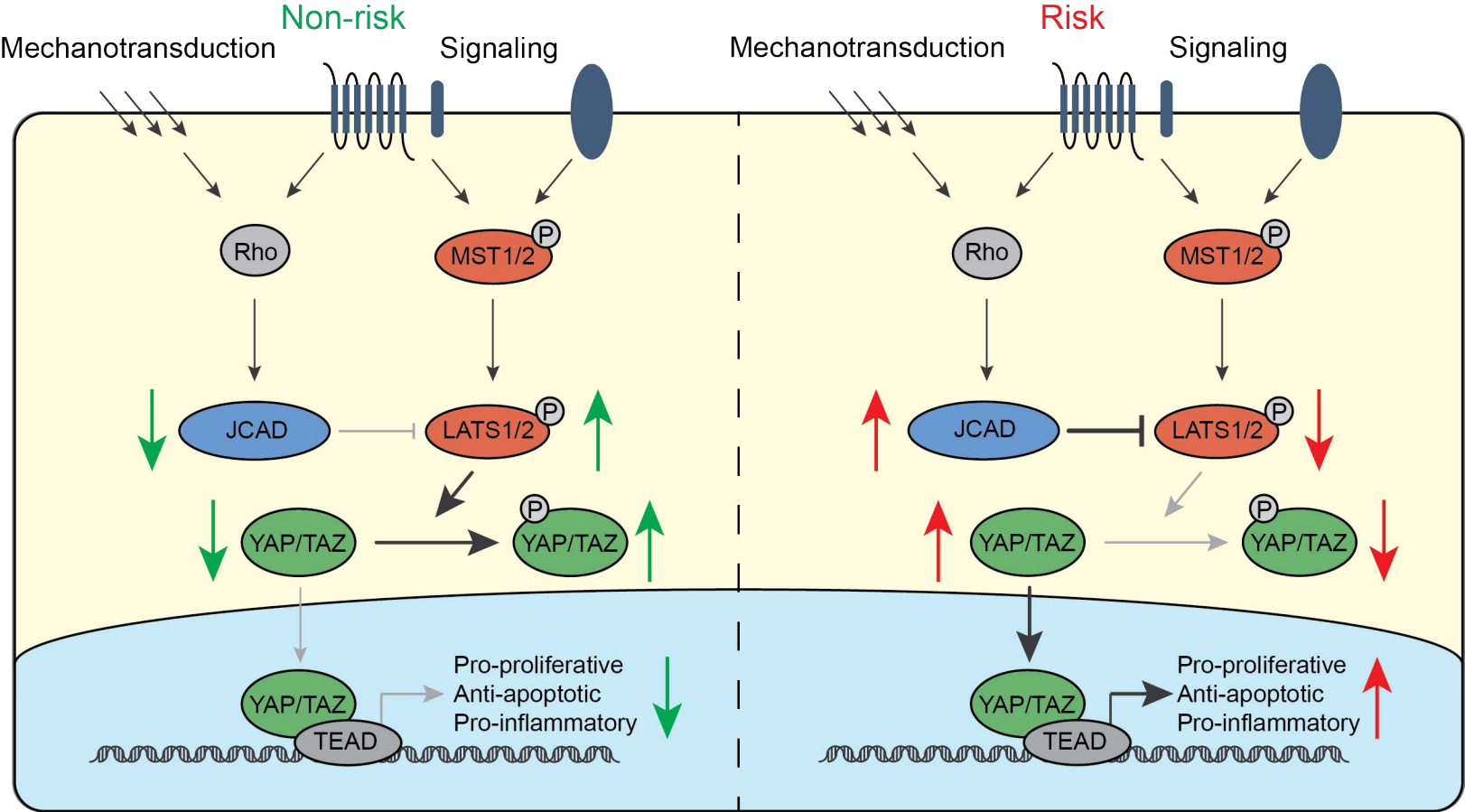
Non-risk
Mechanotransduction
Signaling
Rho
MST1/2
P
JCAD
LATS1/2
P
YAP/TAZ
P
YAP/TAZ
YAP/TAZ
TEAD
Pro-proliferative
Anti-apoptotic
Pro-inflammatory
Risk
Mechanotransduction
Signaling
Rho
MST1/2
P
JCAD
LATS1/2
P
YAP/TAZ
P
YAP/TAZ
YAP/TAZ
TEAD
Pro-proliferative
Anti-apoptotic
Pro-inflammatory

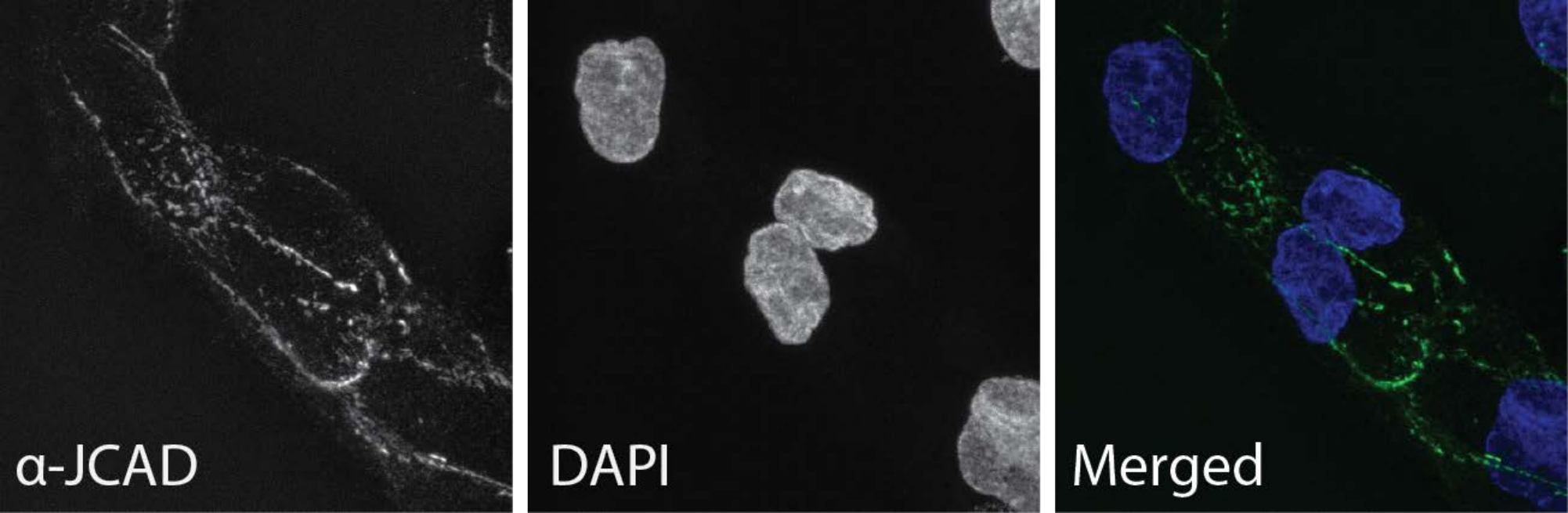
α-JCAD
DAPI
Merged

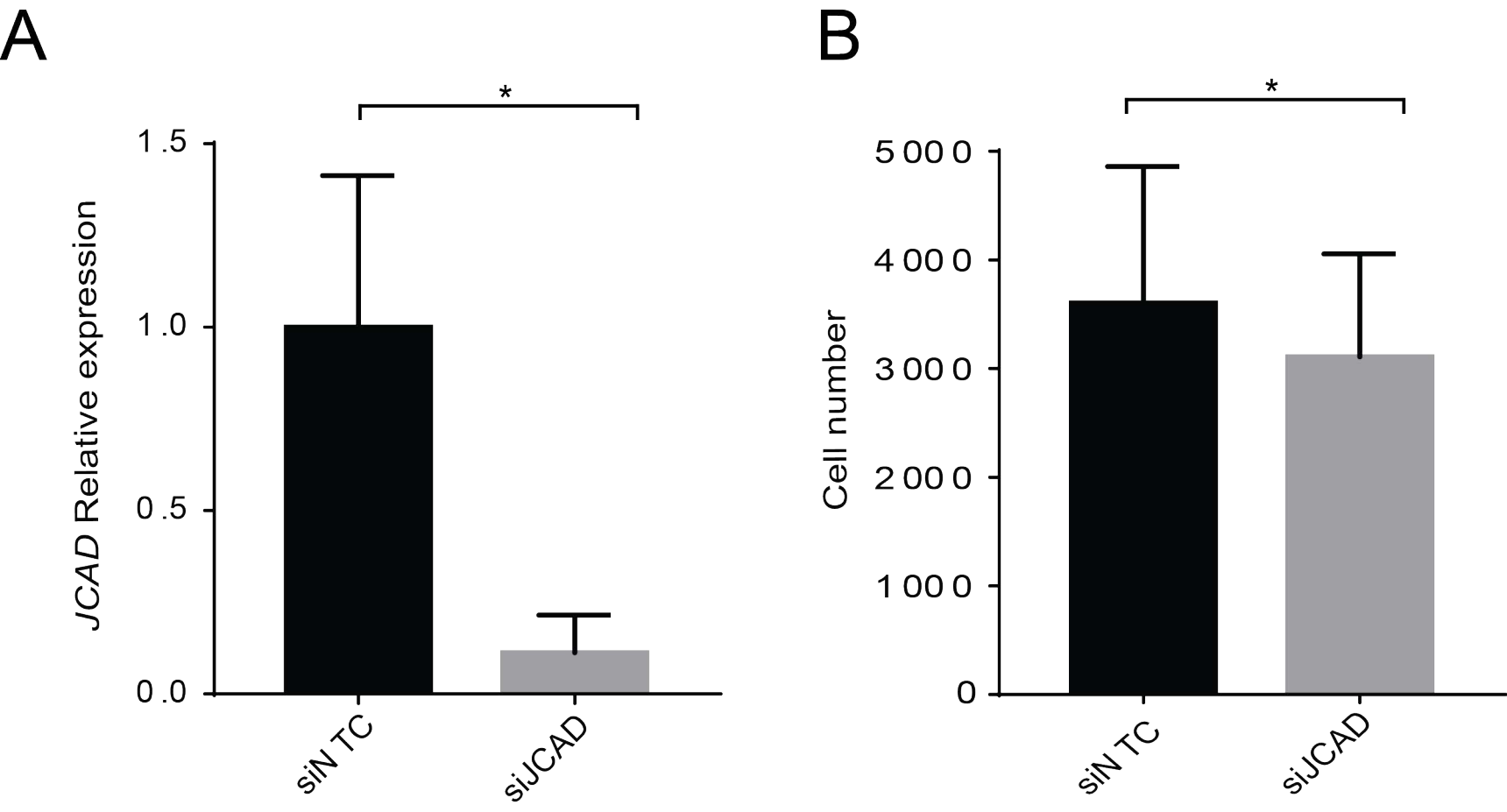
A
*
1.5
1.0
0.5
0.0
JCAD Relative expression
siN TC
siJCAD
B
*
5000
4000
3000
2000
1000
0
Cell number
siN TC
siJCAD

A

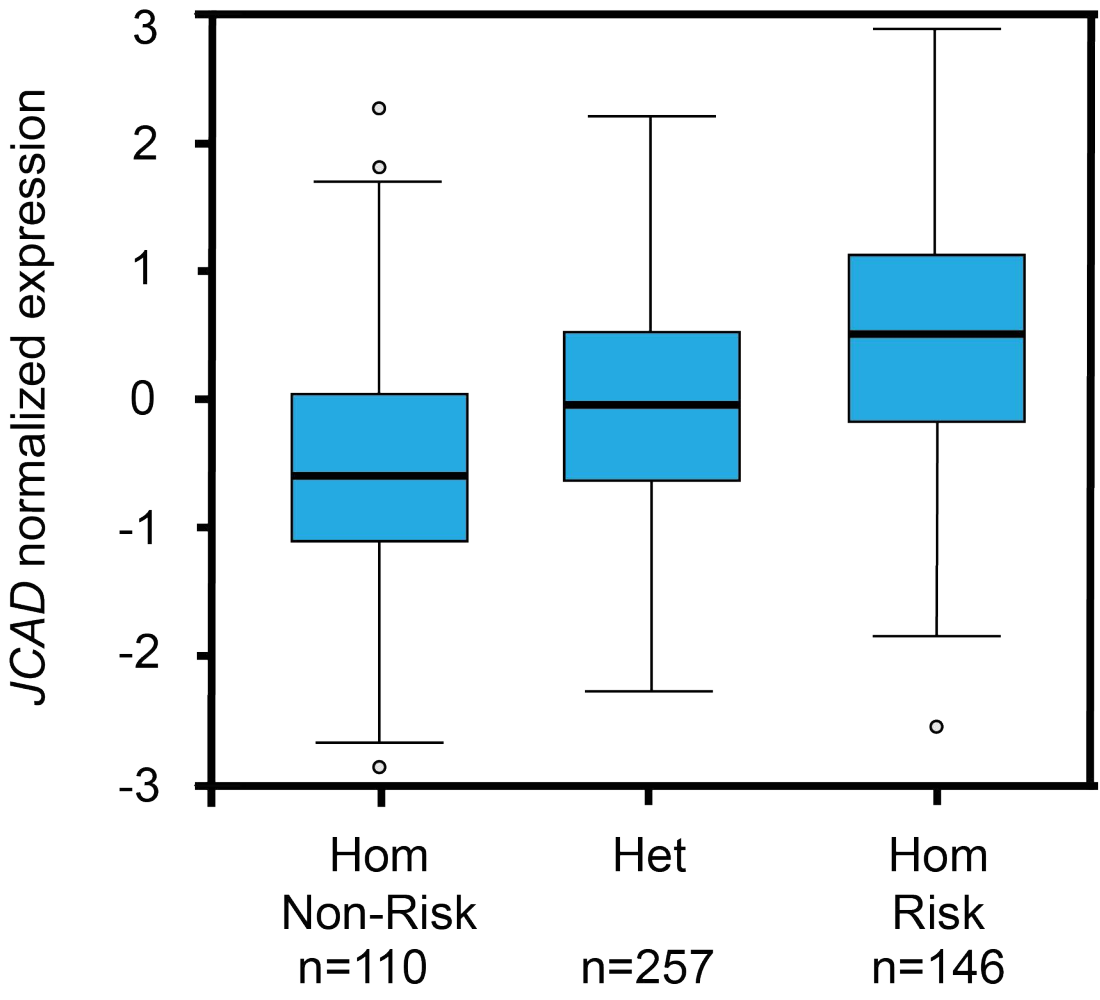
JCAD normalized expression
3
2
1
0
-1
-2
-3
Hom
Non-Risk
n=110
Het
n=257
Hom
Risk
n=146

B

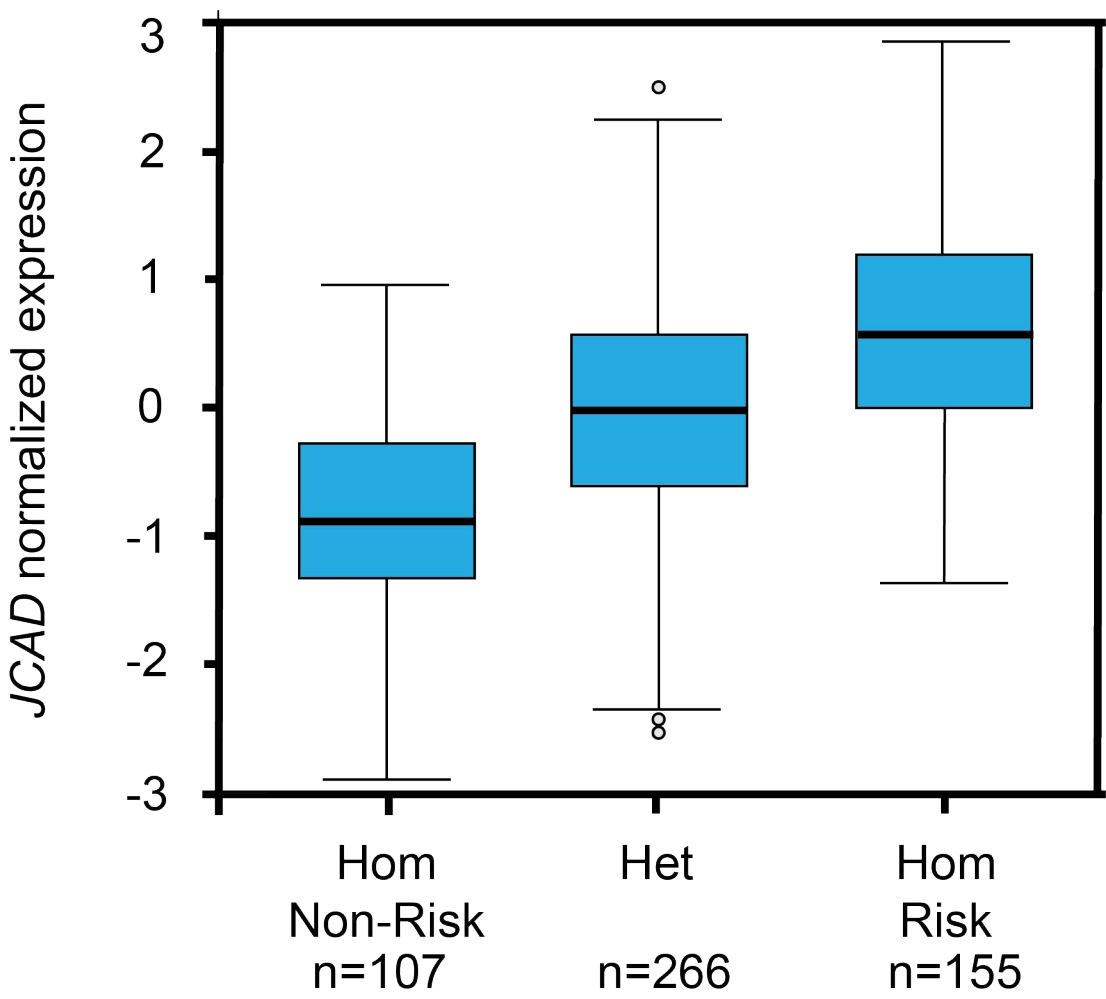
JCAD normalized expression
3
2
1
0
-1
-2
-3
Hom
Non-Risk
n=107
Het
n=266
Hom
Risk
n=155

C

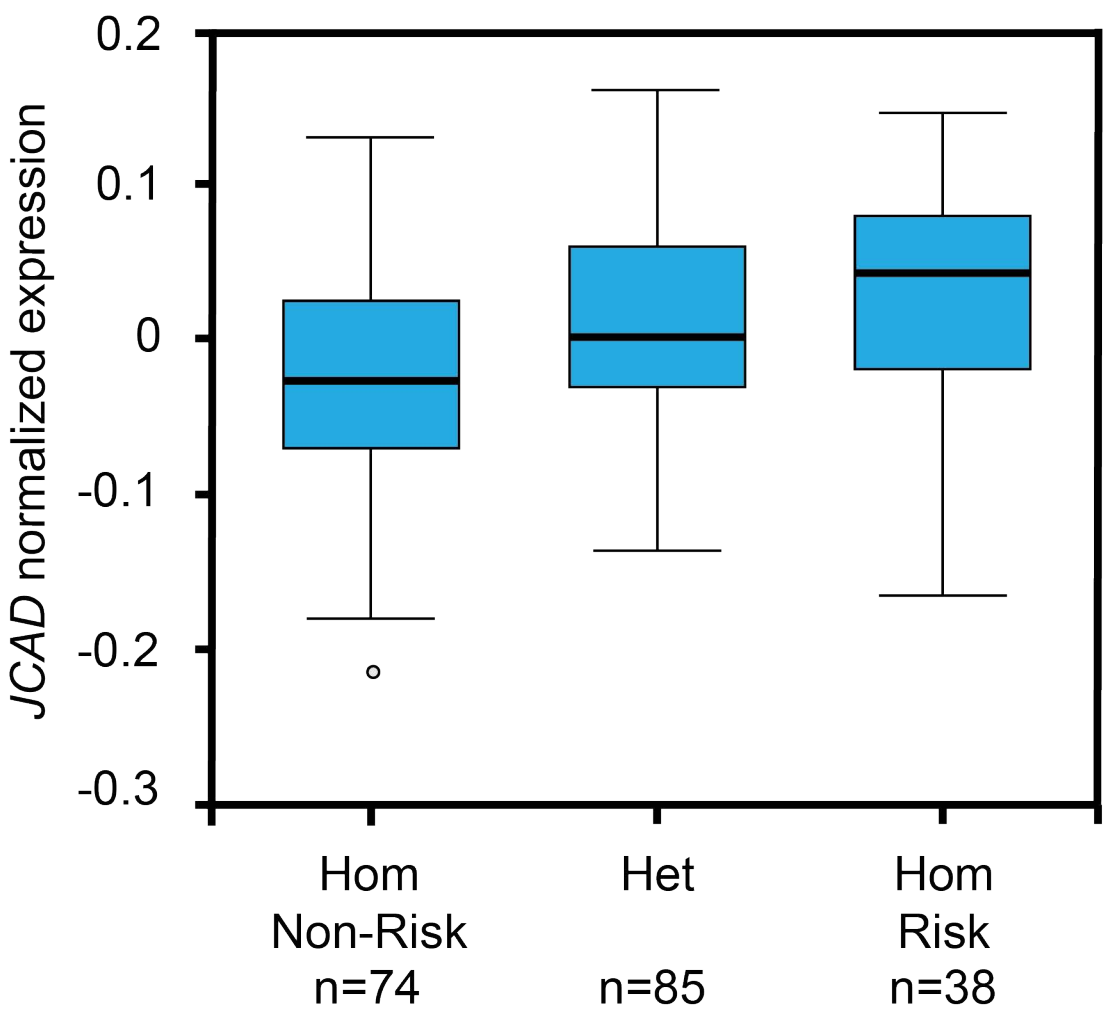
JCAD normalized expression
0.2
0.1
0
-0.1
-0.2
-0.3
Hom
Non-Risk
n=74
Het
n=85
Hom
Risk
n=38

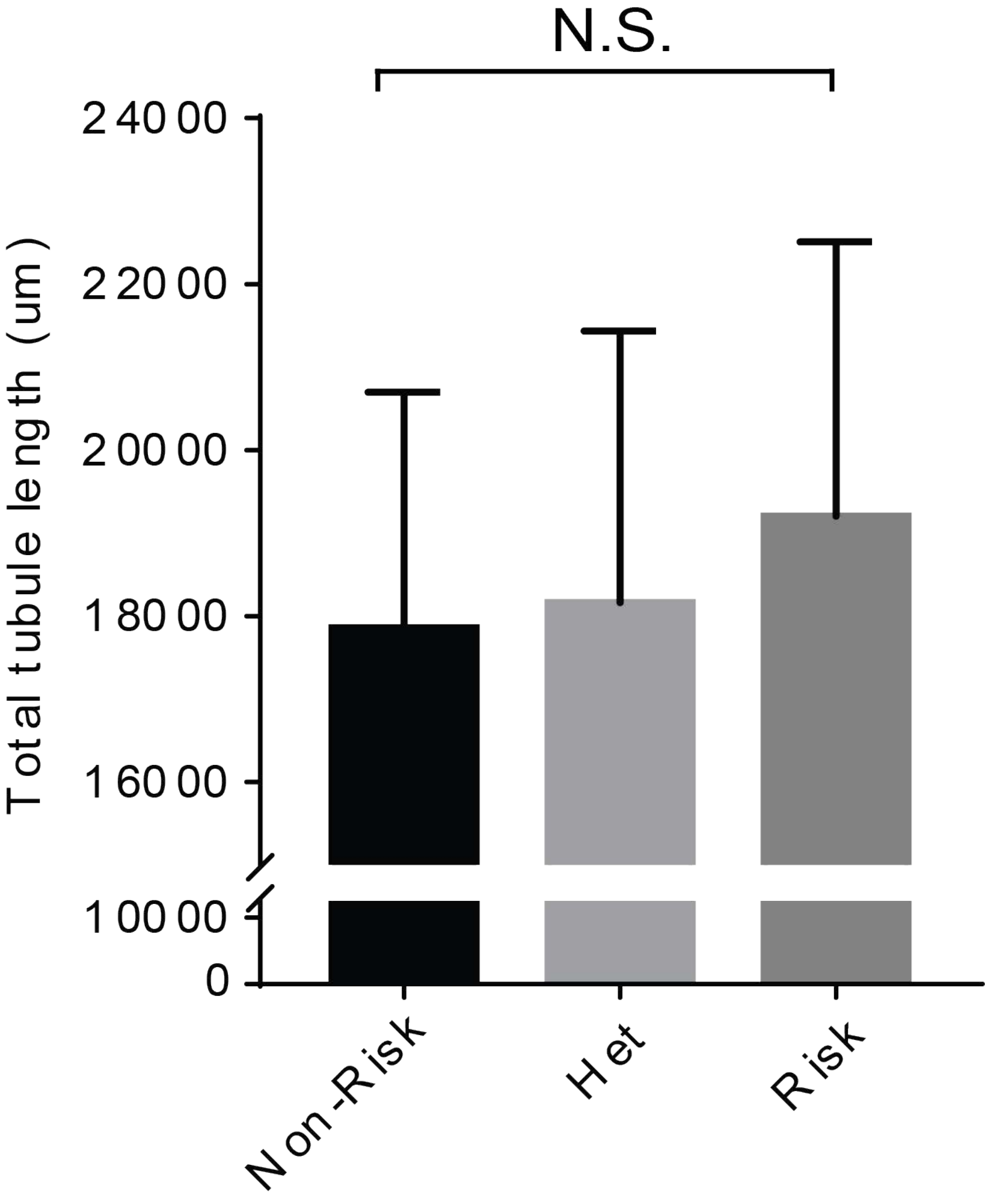
N.S.
2 40 00
2 20 00
2 00 00
1 80 00
1 60 00
1 00 00
0
T ot al t ubule le ng th (um)
N on -R isk
H et
R isk